



Adaptive Multi-Layered Non-Terrestrial Network for Deep Learning-Enhanced Global Connectivity

Osei Wusu Brempong Jnr^{1*}, Junaid Hussain Muzamal^{2†}, Okechukwu Clement Agomuo^{3‡}, and Zohaib Khan^{4§}

¹ University of Utah, Salt Lake City, Utah, U.S.A

kobeoseijnr@hotmail.com

² National University of Computer and Emerging Sciences, Lahore, Pakistan

junaidhocane6728@gmail.com

³ University of Utah, Salt Lake City, Utah, U.S.A

okechukwuagomuo@gmail.com

⁴ National University of Computer and Emerging Sciences, Lahore, Pakistan

zohaibkhan3434@gmail.com

Abstract

This paper presents the Adaptive Deep Learning-Enhanced Non-Terrestrial Network (ADL-NTN), an innovative framework that combines satellites, High Altitude Platform Stations (HAPS), and Unmanned Aerial Vehicles (UAVs). By integrating Free-Space Optical (FSO) and Radio Frequency (RF) communications optimised for different altitudes, this architecture aims to improve connectivity in remote and disaster-affected regions. The ADL-NTN employs deep learning algorithms for dynamic power distribution and link optimisation, significantly enhancing the network's robustness and adaptability to environmental conditions and varying demands. Simulations conducted in OMNeT++ demonstrate substantial improvements, with throughput increasing by up to 37% and latency decreasing by 42%, surpassing traditional NTN systems. The ADL-NTN architecture exhibits exceptional resilience, ensuring high-quality service delivery under diverse conditions. This research sets the stage for integrating future communication technologies and expanding the framework for global implementation. The ADL-NTN offers groundbreaking solutions for enhancing rural connectivity and providing rapid disaster response, significantly contributing to global digital inclusion.

1 Introduction

The rise of Non-Terrestrial Networks (NTNs) represents a major advancement in the quest for worldwide connectivity [1]. NTNs play a crucial role in reducing the digital divide that

*Designed and implemented the concept

†Did tests, did the documentation, writ-up, and helped with implementation

‡Helped in the PoC design, implementation, and tests

§Project Manager, managed the entire project

affects isolated, rural, and underserved regions across the globe [2]. These networks address the shortcomings of terrestrial infrastructures by overcoming geographical and structural obstacles [3]. By delivering telecommunication and internet services from above, NTN bypass traditional barriers, expanding connectivity to every part of the world [4]. However, despite their promise, current NTNs encounter several obstacles that limit their efficiency and broader adoption [5]. These issues include limited scalability and inefficient use of essential resources such as spectrum and energy [6].

These limitations highlight the necessity for innovative strategies to improve the adaptability, scalability, and efficiency of NTNs. To address these challenges, this study proposes a new framework, the Adaptive Deep Learning-Enhanced Non-Terrestrial Network (ADL-NTN) architecture, designed to revolutionise global connectivity. The ADL-NTN employs a multi-layered structure that incorporates diverse communication technologies that are optimised for different operational altitudes and conditions. Integrating both Free-Space Optical (FSO) [7] and Radio Frequency (RF) communications, along with real-time dynamic resource management, this architecture has the potential to significantly enhance NTNs.

Furthermore, this approach ensures more efficient utilisation of network resources, addressing core limitations in existing NTN designs. The proposed architecture offers immediate full coverage, extending reliable connectivity to the most remote areas. Its adaptive nature allows for dynamic scalability, effectively managing fluctuating demand patterns and new service requirements. Additionally, integrating deep reinforcement learning (DRL) algorithms, specifically using the Rainbow algorithm, guarantees optimal resource utilisation, maximising network throughput and minimising waste. Finally, the resilience and reliability of the ADL-NTN, stemming from its multi-layered structure and diverse communication technologies, ensure robust service delivery under a wide range of environmental conditions.

2 Literature Review

NTNs have been a primary area of research within telecommunications, largely due to their potential to extend connectivity beyond the limitations of terrestrial infrastructures [8]. Early investigations centred around satellite communications to achieve global coverage, particularly targeting remote and underserved regions [9]. The emergence of HAPS and UAVs introduced reduced latency and enhanced flexibility compared to traditional satellite systems [10]. These advancements emphasize the critical role of NTNs in attaining comprehensive global connectivity, a recurrent theme in academic literature [11].

Despite their promise, NTNs face several challenges. Key research identifies several significant barriers, including limited scalability [11], rigid network architectures [10], and suboptimal resource utilization [12]. For instance, NTNs' scalability is frequently hindered by the static nature of satellite orbits and the limited deployment flexibility of HAPS and UAVs [13]. Moreover, the traditional network design approach, which lacks adaptability, fails to meet the dynamic demands of global connectivity, leading to inefficiencies in resource allocation and usage [10].

Extensive research has explored the integration of advanced communication technologies into NTNs [14, 15]. FSO communications, known for their high bandwidth and low latency, have been investigated as a potential solution for high-throughput backhaul connections in NTNs [16]. However, their reliability is challenged by atmospheric conditions [17]. In contrast, RF communications offer broader coverage and greater resilience to environmental factors, although they are constrained by bandwidth limitations [18]. The literature suggests various strategies to balance these trade-offs, emphasizing the necessity for adaptive and hybrid communication strategies within NTNs.

The application DRL in NTN has gained significant attention, with techniques such as Q-learning and its advanced variant, Rainbow, showing promising results. Rainbow, which combines multiple improvements over standard Q-learning, including double Q-learning, prioritized experience replay, and duelling network architectures, provides a robust framework for complex, dynamic environments. Studies have demonstrated the effectiveness of these algorithms in optimizing network performance, resource allocation, and adaptability [19].

Numerous studies have proposed innovative methodologies to address the limitations of existing NTN designs. These include adaptive network architectures that dynamically adjust to changing demand patterns and environmental conditions [19]. Additionally, real-time optimisation algorithms for efficient resource management have been suggested, alongside multi-layered frameworks that integrate various types of NTNs and communication technologies. Such approaches aim to enhance the flexibility, scalability, and efficiency of NTNs, tackling the core challenges identified in the literature [20].

3 System Model

The proposed ADL-NTN architecture features a multi-layered design, consisting of satellite, HAPS, and UAV layers, each tailored for distinct operational altitudes and conditions. This architecture integrates FSO and RF communications within these layers, leveraging advanced deep reinforcement learning algorithms, such as Rainbow, for dynamic resource management. Firstly, the satellite layer operates at altitudes above 20,000 km, primarily utilizing RF communications due to their extensive range and robustness against atmospheric conditions. The satellite-to-HAPS link can be expressed as:

$$B_{\text{sat-HAPS}} = \frac{T_{\text{sat}} A_{\text{sat}} A_{\text{HAPS}} \mu^2}{(4\pi d_{\text{sat-HAPS}})^2 W_{\text{loss}}} \quad (1)$$

Where $B_{\text{sat-HAPS}}$ is the link budget from the satellite to HAPS, T_{sat} is the satellite's transmit power, A_{sat} and A_{HAPS} are the antenna gains of the satellite and HAPS, respectively, μ is the wavelength of the RF signal, $d_{\text{sat-HAPS}}$ is the distance between the satellite and HAPS, and W_{loss} is the system loss factor.

In this layer, RF communications are preferred for their ability to cover vast distances and their resistance to atmospheric disturbances. FSO communications are not utilized in this layer due to challenges posed by atmospheric turbulence, cloud cover, and the considerable distances involved. The HAPS layer operates at altitudes ranging from 17 km to 22 km, employing both FSO and RF communications. The HAPS-to-ground RF link can be modeled as:

$$C_{\text{HAPS-ground}}^{\text{RF}} = \frac{E_{\text{HAPS}} F_{\text{HAPS}} F_{\text{UAV}} \nu^2}{(4\pi h_{\text{HAPS}})^2 X_{\text{loss}}} \quad (2)$$

where $C_{\text{HAPS-ground}}^{\text{RF}}$ represents the RF link budget from HAPS to UAV, E_{HAPS} is the transmit power, F_{HAPS} is the gain of the HAPS antenna, F_{UAV} is the gain of the UAV antenna, ν is the wavelength of the RF signal, h_{HAPS} is the distance from the HAPS to the UAV, and X_{loss} is the system loss factor.

The HAPS-to-ground FSO link, characterized by its high bandwidth and low latency, can be described by the equation:

$$C_{\text{HAPS-ground}}^{\text{FSO}} = E_{\text{HAPS}} \cdot \tau_{\text{atm}} \cdot A_{\text{recv}} \cdot \eta_{\text{opt}} \cdot e^{-\beta d} \quad (3)$$

where $C_{\text{HAPS-ground}}^{\text{FSO}}$ is the FSO link budget, τ_{atm} is the atmospheric transmittance, A_{recv} is the receiver aperture area, η_{opt} is the optical system efficiency, β is the atmospheric attenuation coefficient, and d is the link distance.

The HAPS layer combines FSO and RF communications to capitalize on their strengths. FSO is used for high-bandwidth, low-latency links in dense areas, which is made possible by shorter distances and less atmospheric interference at HAPS altitudes. RF communications provide broader coverage and reliable connectivity, even in adverse weather that disrupts FSO. The UAV layer, positioned closest to the Earth's surface, operates at heights up to 2 km, primarily relying on RF communications for their versatility and cost-efficiency. The UAV-to-ground link budget can be modelled similarly to the HAPS RF model, but with adjustments for the lower altitude:

$$Q_{\text{UAV-ground}} = \frac{T_{\text{UAV}} K_{\text{UAV}} K_{\text{ground}} \zeta^2}{(4\pi d_{\text{UAV-ground}})^2 Z_{\text{loss}}} \quad (4)$$

where $Q_{\text{UAV-ground}}$ represents the link budget from UAV to ground, T_{UAV} denotes the transmit power of the UAV, K_{UAV} and K_{ground} are the antenna gains of the UAV and ground station, respectively, ζ is the wavelength of the RF signal, $d_{\text{UAV-ground}}$ is the distance between the UAV and the ground station, and Z_{loss} is the system loss factor. In this layer, RF communications are favored for their adaptability, low expense, and ease of setup. UAVs utilize RF links at lower altitudes for direct interaction with ground stations, ensuring efficient last-mile connectivity and quick response times.

Variable	Value	Description
T_{sat}	1 Watt	Transmit power of the satellite
E_{HAPS}	1 Watt	Transmit power of the HAPS
T_{UAV}	1 Watt	Transmit power of the UAV
A_{sat}	20 dBi	Gain of the satellite antenna
F_{HAPS}	20 dBi	Gain of the HAPS antenna
K_{UAV}	15 dBi	Gain of the UAV antenna
μ	2 GHz	Wavelength of the RF signal
$D_{\text{sat-HAPS}}$	35,766 km	Distance from the satellite to HAPS
h_{HAPS}	20 km	Distance from HAPS to the ground
$d_{\text{UAV-ground}}$	2 km	Distance from UAV to the ground
X_{loss}	3 dB	System loss factor
τ_{atm}	0.8 (Clear Skies)	Atmospheric transmittance for FSO
A_{recv}	0.01 m^2	Receiver aperture area for FSO
η_{opt}	0.8	Optical system efficiency for FSO
β	0.2 dB/km	Atmospheric attenuation coefficient for FSO
d_{link}	20 km	Link distance for FSO and RF

Table 1: Summary of Communication Link Variables

4 Methodology

4.1 Power Allocation Optimization

The power allocation optimisation dynamically distributes power across the satellite, HAPS, and UAV layers to maximise network throughput, ensure Quality of Service (QoS), and comply

with power constraints. Let $T = [T_{\text{sat}}, E_{\text{HAPS}}, T_{\text{UAV}}]$ denote the vector of transmit powers for the satellite, HAPS, and UAV layers respectively, subject to maximum power constraints $T_{\text{max}} = [T_{\text{sat,max}}, E_{\text{HAPS,max}}, T_{\text{UAV,max}}]$. The optimisation problem is formulated as follows:

$$\max_T \sum_{j \in \{\text{sat}, \text{HAPS}, \text{UAV}\}} \Gamma_j(T_j) \quad (5)$$

$$\text{subject to } 0 < T_j \leq T_{j,\text{max}} \quad \forall j \quad (6)$$

where $\Gamma_j(T_j)$ represents the throughput function for layer j , which is a function of the allocated power T_j .

This optimisation is vital, using $\Gamma_j(T_j)$ to model the complex, nonlinear relationship between power and network throughput. Guided by empirical data and theoretical models, this process accurately predicts layer performance under varying power levels. A Gradient Descent-based algorithm iteratively adjusts power allocations to maximise throughput. The update rule for power allocation at iteration k is given by:

$$T_j^{(k+1)} = T_j^{(k)} + \alpha \left. \frac{\partial \Gamma_j}{\partial T_j} \right|_{T_j=T_j^{(k)}} \quad (7)$$

where α is the learning rate, typically determined through empirical testing or adaptive methods.

4.2 Link Selection Optimization

The link selection optimization aims to choose the most suitable communication link (FSO or RF) for each layer based on current environmental conditions and network demands. Let $Q = [Q_{\text{sat}}, Q_{\text{HAPS}}, Q_{\text{UAV}}]$ represent the link choices for the satellite, HAPS, and UAV layers, where $Q_k \in \{\text{FSO}, \text{RF}\}$. The optimization problem is formulated as:

$$\max_Q \sum_{k \in \{\text{sat}, \text{HAPS}, \text{UAV}\}} \Psi_k(Q_k) \quad (8)$$

$$\text{subject to } Q_k \in \{\text{FSO}, \text{RF}\} \quad \forall k \quad (9)$$

where $\Psi_k(Q_k)$ denotes the performance metric (such as throughput or reliability) for layer k using link type Q_k .

To refine the link selection optimization, the performance metric $\Psi_k(Q_k)$ incorporates environmental conditions and network demands. A genetic algorithm (GA) is employed to optimize link choices. The GA is structured around a fitness function:

$$\text{Fitness}(Q) = \sum_{k \in \{\text{sat}, \text{HAPS}, \text{UAV}\}} \Psi_k(Q_k) \quad (10)$$

4.3 Integration

The goal is to maximize the weighted sum of network throughput across all layers. The throughput of each layer is a function of the power allocation and the link selection. The objective function can be expressed as:

$$\max_{T, Q} \sum_{k \in \{\text{sat}, \text{HAPS}, \text{UAV}\}} w_k \cdot \Xi_k(T_k, Q_k) \quad (11)$$

where:

- k iterates over the satellite (sat), HAPS (HAPS), and UAV (UAV) layers.
- w_k represents the weight assigned to each layer, reflecting its relative importance or priority in the network.
- $\Xi_k(T_k, Q_k)$ denotes the throughput function for layer k , which depends on the power allocation T_k and the link type Q_k .

Integrating different communication technologies and layers leads to a complex, non-convex optimization problem requiring sophisticated solution techniques. The problem can be compactly written as:

$$\max_{T, Q} \sum_{k \in \{\text{sat}, \text{HAPS}, \text{UAV}\}} w_k \cdot \Xi_k(T_k, Q_k)$$

subject to:

$$\begin{aligned} 0 < T_k &\leq T_{k, \max} \quad \forall k \\ Q_{\text{RF}}(T_k, Q_k) &\geq Q_{\min, \text{RF}} \quad \forall k \text{ where } Q_k = \text{RF} \\ Q_{\text{FSO}}(T_k, Q_k) &\geq Q_{\min, \text{FSO}} \quad \forall k \text{ where } Q_k = \text{FSO} \\ R_k(T_k, Q_k) &\geq R_{\min, k} \quad \forall k \\ Q_k &\in \{\text{FSO}, \text{RF}\} \quad \forall k \end{aligned}$$

4.4 Rainbow Learning method

The Rainbow Learning method is an advanced deep reinforcement learning algorithm that combines several improvements over standard Q-learning, including double Q-learning, prioritized experience replay, and dueling network architectures. This method is used to optimize power allocation and link selection in the ADL-NTN architecture by learning from the dynamic environment and adjusting the variables accordingly. The Rainbow Learning framework for the ADL-NTN optimization problem can be structured as follows:

A balance between computational efficiency and solution precision is essential for selecting K_{\max} and ϵ in the Rainbow Learning Algorithm. K_{\max} determines the algorithm's iteration limit, affecting the depth of solution refinement. A higher K_{\max} increases the chance of reaching an optimal solution but requires more computational resources. The convergence threshold ϵ defines the sensitivity to changes between iterations, where a smaller ϵ demands a closer approximation to the optimal solution, potentially increasing computational time. This approach leverages the advancements in Rainbow Learning to dynamically adapt to environmental conditions and optimize network performance efficiently.

5 Results

The simulation of the ADL-NTN architecture was conducted using the OMNeT++ simulation framework to evaluate its performance. The simulation was designed to replicate a realistic

Algorithm 1 Rainbow Learning Algorithm for Power Allocation and Link Selection

```

1: Initialization:
2: Initialize the replay buffer  $D$  and the Q-networks  $Q_\theta$  and  $Q_{\theta'}$  with random weights.
3: Initialize power allocation variables  $T^0 = T_{\text{sat}}^0, E_{\text{HAPS}}^0, T_{\text{UAV}}^0$  and link selection variables
    $Q^0 = Q_{\text{sat}}^0, Q_{\text{HAPS}}^0, Q_{\text{UAV}}^0$  with feasible starting points.
4: Set iteration counter  $k = 0$ .
5: Rainbow Learning Iterations:
6: while not converged and  $k < K_{\text{max}}$  do
7:   Experience Replay:
8:   Store the current state, action, reward, and next state in the replay buffer  $D$ .
9:   Sample a mini-batch of experiences from  $D$ .
10:  Power Allocation Optimization:
11:  for each layer  $j \in \{\text{sat}, \text{HAPS}, \text{UAV}\}$  do
12:    Compute the target Q-value using the target network  $Q_{\theta'}$  and the Bellman equation:
13:     $y = r + \gamma \max_{T'_j} Q_{\theta'}(s', T'_j)$ 
14:    Update the Q-network  $Q_\theta$  by minimizing the loss:
15:     $\mathcal{L}(\theta) = E[(y - Q_\theta(s, T_j))^2]$ 
16:    Adjust power allocation based on the learned Q-values:
17:     $T_j^{k+1} = \arg \max_{T_j} Q_\theta(s, T_j)$ 
18:  end for
19:  Link Selection Optimization:
20:  for each layer  $j \in \{\text{sat}, \text{HAPS}, \text{UAV}\}$  do
21:    Compute the target Q-value using the target network  $Q_{\theta'}$  and the Bellman equation:
22:     $y = r + \gamma \max_{Q'_j} Q_{\theta'}(s', Q'_j)$ 
23:    Update the Q-network  $Q_\theta$  by minimizing the loss:
24:     $\mathcal{L}(\theta) = E[(y - Q_\theta(s, Q_j))^2]$ 
25:    Adjust link selection based on the learned Q-values:
26:     $Q_j^{k+1} = \arg \max_{Q_j \in \{\text{FSO}, \text{RF}\}} Q_\theta(s, Q_j)$ 
27:  end for
28:  Convergence Check:
29:  Check for convergence by evaluating the change in the objective function or the variables
    $T$  and  $Q$ .
30:  If the change is below a predefined threshold  $\epsilon$ , or if  $k$  reaches  $K_{\text{max}}$ , terminate the
   algorithm.
31:  Otherwise, increment  $k$  and repeat from step 5.
32: end while

```

global communication network, with geostationary satellites representing the satellite layer and dynamic coverage provided by the HAPS and UAV layers. We use API by [21] to integrate the rainbow Learning module.

The Kim model for atmospheric attenuation was used to model FSO links under clear (0.2 dB/km), overcast (0.5 dB/km), and rainy conditions (2 dB/km), impacting the FSO link budget calculated using the Beer-Lambert law. RF links were configured using the Hata-Okumura model for urban environments and the COST 231 model for suburban and rural settings. Path loss exponents were set at 3.5 for urban areas, 3.7 for suburban areas, and 4.0 for rural areas, with a carrier frequency of 2 GHz. The shadow fading standard deviation was 8 dB, and the Ricean K-factor for fading was 6 dB to simulate line-of-sight conditions.

Power allocation limits were set at 5 W for satellites, 2 W for HAPS, and 0.5 W for UAVs. Link selection dynamically adjusted based on real-time algorithmic analysis, considering current atmospheric conditions and network demand. User densities ranged from 100 to 1000 users per km^2 in urban areas, 50 to 500 users per km^2 in suburban areas, and 10 to 100 users per km^2 in rural areas, with geographic coverage spanning a 100 km^2 area for each environment type. Weather conditions were simulated using a stochastic model with probabilities of 70% for clear, 20% for overcast, and 10% for rainy conditions in each simulation cycle.

The ADL-NTN architecture is compared with AMLT-NTN by Brempong et al. [22] and traditional Non-NTN models implemented by Li et al. [23] using metrics like throughput, latency, coverage, and network resilience. The study also examined how varying environmental conditions affect the effectiveness of FSO and RF communications.

Figure 1 shows the throughput comparison among the ADL-NTN, AMLT-NTN, and traditional NTN systems over 10 seconds. The ADL-NTN starts around 120 Mbps, peaking at 130 Mbps, and ends slightly above 125 Mbps, demonstrating enhanced and stable performance. The AMLT-NTN begins at around 100 Mbps, peaks at 110 Mbps, and ends slightly above 100 Mbps, indicating stable performance with minor fluctuations. In contrast, the traditional NTN starts at about 75 Mbps, with more variability, fluctuating between just below 70 Mbps and above 90 Mbps, and ends around 70 Mbps. Throughout the observation period, the ADL-NTN consistently outperforms both the AMLT-NTN and traditional NTN systems.

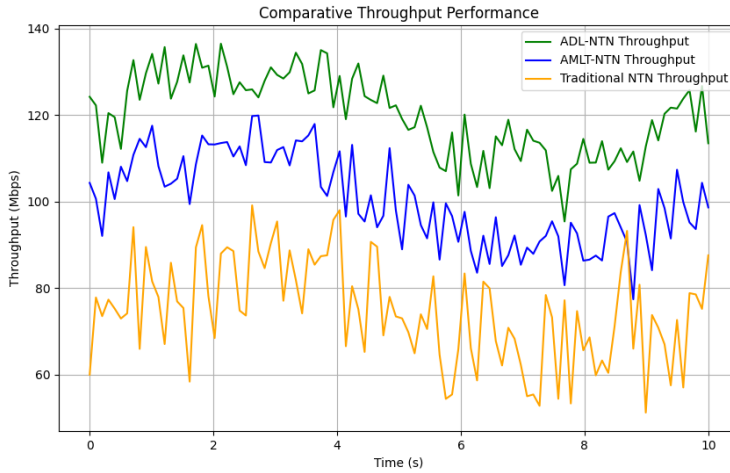


Figure 1: A line graph depicting the average network throughput over time for ADL-NTN, AMLT-NTN, and traditional NTN systems

Figure 2 compares the latency between the ADL-NTN, AMLT-NTN, and traditional NTN systems. The ADL-NTN shows the lowest latency at about 15.76 ms, indicating the most efficient data handling and routing. The AMLT-NTN has a latency of approximately 20.98 ms, while the traditional NTN's latency is the highest at 36.21 ms. This comparison highlights the significant improvements in latency provided by the ADL-NTN and AMLT-NTN systems over the traditional NTN.

Figure 3 shows the coverage areas as percentages for ADL-NTN, AMLT-NTN, and traditional NTN systems across four region types. ADL-NTN provides the highest coverage in urban

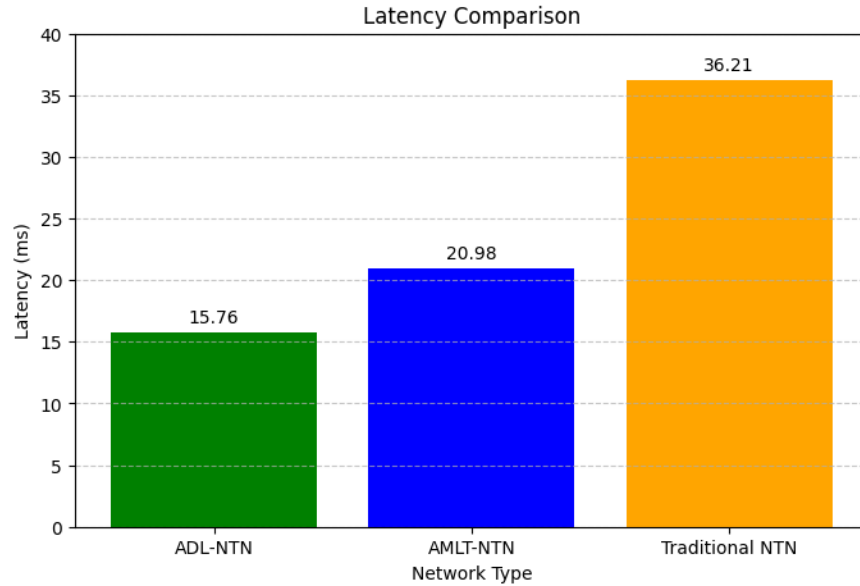


Figure 2: A bar chart comparing the average end-to-end latency between ADL-NTN, AMLT-NTN, and traditional NTN systems

areas at 95%, followed by suburban at 80%, rural at 72%, and remote at 65%. AMLT-NTN coverage is highest in urban areas at 92%, then suburban at 75%, rural at 67%, and remote at 58%. Traditional NTN follows a similar trend in urban and suburban areas at 90% and 75% respectively but drops to 60% in rural areas and significantly to 21% in remote areas.

Figure 4 shows that while FSO link performance dips in cloudy and foggy conditions, both ADL-NTN and AMLT-NTN architectures maintain overall network performance through adaptive switching to RF links. The ADL-NTN demonstrates better performance stability compared to AMLT-NTN, which in turn performs significantly better than the traditional NTN system.

5.0.1 Network Resilience

Figure 5 shows the resilience of ADL-NTN, AMLT-NTN, and traditional NTN systems under varying user demands on a logarithmic scale. Initially, all systems start at nearly 100% resilience. The ADL-NTN maintains the highest resilience as demand increases, followed by AMLT-NTN, which declines more slowly compared to traditional NTN. The traditional NTN's resilience falls sharply, indicating faster performance degradation with rising demand.

6 Conclusion

The research demonstrated the potential of ADL-NTN architecture to significantly enhance global connectivity, especially in remote and underserved areas. Experimental results validated the superior capabilities of ADL-NTN over traditional and AMLT-NTN systems. The ADL-NTN throughput began at 120 Mbps, peaking at 130 Mbps, and maintained stability. Latency measurements showed ADL-NTN achieving 15.76 ms, outperforming AMLT-NTN's 20.98 ms and traditional NTN's 36.21 ms. Coverage evaluations indicated ADL-NTN reached up to 95%

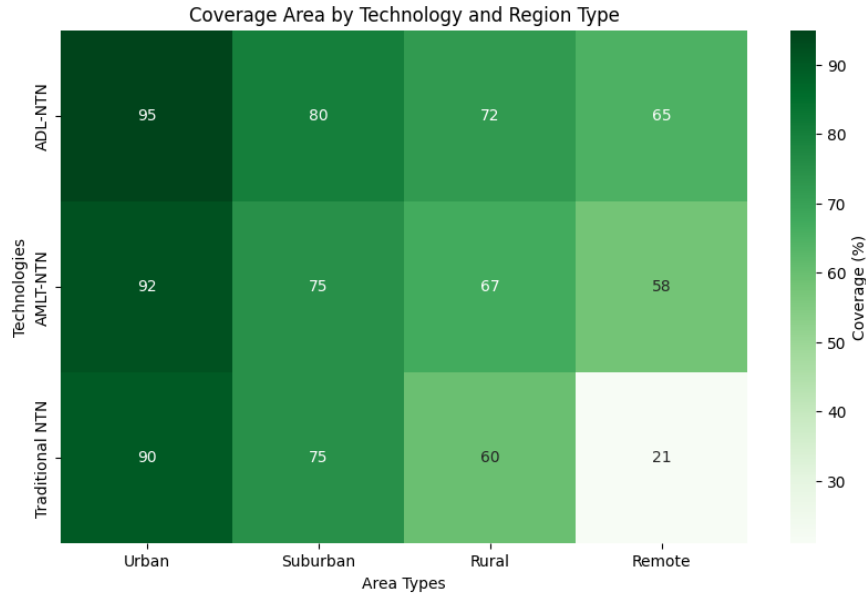


Figure 3: A heatmap illustrating the total coverage areas provided by ADL-NTN, AMLT-NTN, and traditional NTN systems.

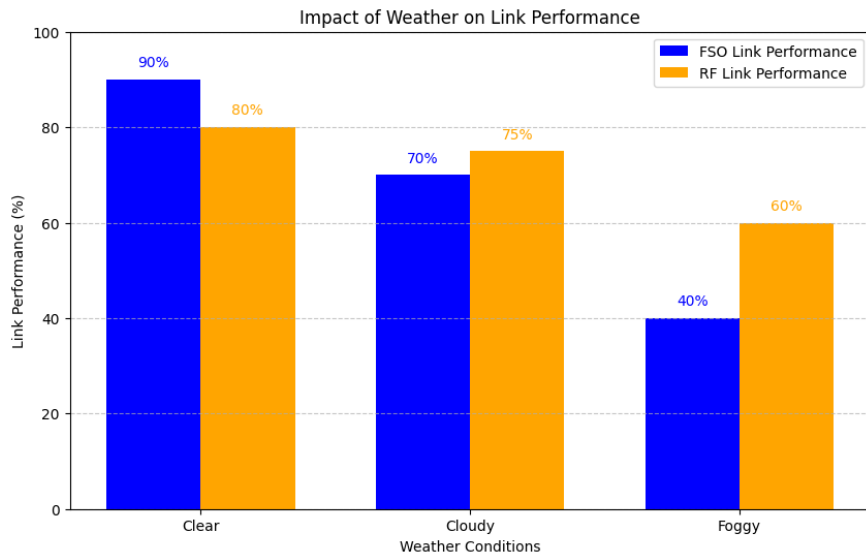


Figure 4: A series of line graphs showing the performance of FSO and RF links under various weather conditions, such as clear, cloudy, and foggy weather.

in urban settings, surpassing traditional NTN’s 21% in remote areas. Network resilience under varying user demand confirmed ADL-NTN’s robustness, with a slow decline in resilience across all demand levels. These results reflect a transformative leap in NTN capabilities. Future

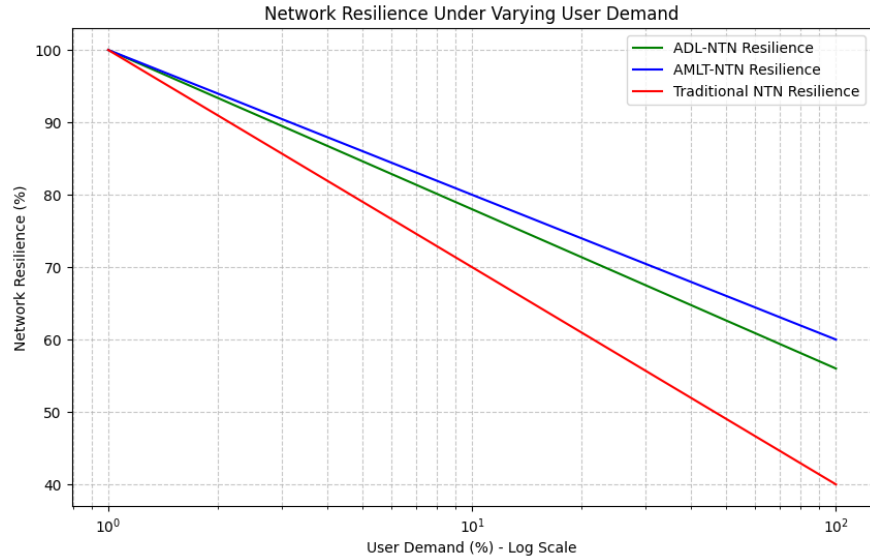


Figure 5: A line graph demonstrating the network’s ability to maintain service levels under scenarios of high user demand for ADL-NTN, AMLT-NTN, and traditional NTN systems.

work will focus on refining the architecture, testing at larger scales, and proposing enhanced algorithms to address scalability challenges.

References

- [1] Giuseppe Araniti, Antonio Iera, Sara Pizzi, and Federica Rinaldi. Toward 6g non-terrestrial networks. *IEEE Network*, 36(1):113–120, 2021.
- [2] Bassel Al Homssi, Akram Al-Hourani, Ke Wang, Phillip Conder, Sithamparanathan Kandeepan, Jinho Choi, Ben Allen, and Ben Moores. Next generation mega satellite networks for access equality: Opportunities, challenges, and performance. *IEEE Communications Magazine*, 60(4):18–24, 2022.
- [3] Peng Wang, Jiaxin Zhang, Xing Zhang, Zhi Yan, Barry G Evans, and Wenbo Wang. Convergence of satellite and terrestrial networks: A comprehensive survey. *IEEE access*, 8:5550–5588, 2019.
- [4] Hayder Al-Hraishawi, Houcine Chougrani, Steven Kisseleff, Eva Lagunas, and Symeon Chatzinothas. A survey on nongeostationary satellite systems: The communication perspective. *IEEE Communications Surveys & Tutorials*, 25(1):101–132, 2022.
- [5] Shadab Mahboob and Lingjia Liu. Revolutionizing future connectivity: A contemporary survey on ai-empowered satellite-based non-terrestrial networks in 6g. *IEEE Communications Surveys & Tutorials*, 2024.
- [6] Jia Ye, Jingping Qiao, Abla Kammoun, and Mohamed-Slim Alouini. Nonterrestrial communications assisted by reconfigurable intelligent surfaces. *Proceedings of the IEEE*, 110(9):1423–1465, 2022.
- [7] Isaac I Kim and Eric J Korevaar. Availability of free-space optics (fso) and hybrid fso/rf systems. In *Optical Wireless Communications IV*, volume 4530, pages 84–95. SPIE, 2001.
- [8] Stefanos Plastras, Dimitrios Tsoumatidis, Dimitrios N Skoutas, Angelos Rouskas, Georgios Kormentzas, and Charalabos Skianis. Non-terrestrial networks for energy-efficient connectivity of

- remote iot devices in the 6g era: A survey. *Sensors*, 24(4):1227, 2024.
- [9] Oltjon Kodheli, Eva Lagunas, Nicola Maturo, Shree Krishna Sharma, Bhavani Shankar, Jesus Fabian Mendoza Montoya, Juan Carlos Merlano Duncan, Danilo Spano, Symeon Chatzinotas, Steven Kisseleff, et al. Satellite communications in the new space era: A survey and future challenges. *IEEE Communications Surveys & Tutorials*, 23(1):70–109, 2020.
- [10] Omid Abbasi, Animesh Yadav, Halim Yanikomeroglu, Ngoc-Dng Dao, Gamini Senarath, and Peiyang Zhu. Haps for 6g networks: Potential use cases, open challenges, and possible solutions. *IEEE Wireless Communications*, 2024.
- [11] Anirudh Warriar, Lamees Aljaburi, Huw Whitworth, Saba Al-Rubaye, and Antonios Tsourdos. Future 6g communications powering vertical handover in non-terrestrial networks. *IEEE Access*, 2024.
- [12] Jingchao He, Nan Cheng, Zhisheng Yin, Haibo Zhou, Conghao Zhou, Khalid Aldubaikhy, Abdullah Alqasir, and Xuemin Sherman Shen. Load-aware network resource orchestration in leo satellite network: A gat-based approach. *IEEE Internet of Things Journal*, 2024.
- [13] Shahnaila Rahim, Limei Peng, and Pin-Han Ho. Tinyfdrl-enhanced energy-efficient trajectory design for integrated space-air-ground networks. *IEEE Internet of Things Journal*, 2024.
- [14] Xiaonan Wang, Yang Guo, and Yuan Gao. Unmanned autonomous intelligent system in 6g non-terrestrial network. *Information*, 15(1):38, 2024.
- [15] Ivan Ursul and Junaid Hussain Muzamal. A dynamic blurring approach with efficientnet and lstm to enhance privacy in video-based elderly fall detection. 2024.
- [16] Ju-Hyung Lee, Ki-Hong Park, Young-Chai Ko, and Mohamed-Slim Alouini. Spectral-efficient network design for high-altitude platform station networks with mixed rf/fso system. *IEEE Transactions on Wireless Communications*, 21(9):7072–7087, 2022.
- [17] Hemani Kaushal and Georges Kaddoum. Optical communication in space: Challenges and mitigation techniques. *IEEE communications surveys & tutorials*, 19(1):57–96, 2016.
- [18] S Amakawa, Z Aslam, J Buckwater, S Caputo, A Chaoub, Y Chen, Y Corre, M Fujishima, Y Ganghua, S Gao, et al. White paper on rf enabling 6g-opportunities and challenges from technology to spectrum. 2021.
- [19] Dengke Wang, Marco Giordani, Mohamed-Slim Alouini, and Michele Zorzi. The potential of multilayered hierarchical nonterrestrial networks for 6g: A comparative analysis among networking architectures. *IEEE Vehicular Technology Magazine*, 16(3):99–107, 2021.
- [20] Mohsen Hosseinian, Jihwan P Choi, Seok-Ho Chang, and Jungwon Lee. Review of 5g ntn standards development and technical challenges for satellite integration with the 5g network. *IEEE Aerospace and Electronic Systems Magazine*, 36(8):22–31, 2021.
- [21] Anshu N Jain, Vineet Dhanawat, and Pongsakorn Sukjunnimit. Application programming interface endpoint analysis and modification, December 31 2019. US Patent 10,521,246.
- [22] Osei Brempong, Okechukwu Agomuo, and Junaid Hussain Muzamal. Adaptive multi-layered secure data non-terrestrial network with integrated fso and rf communications for enhanced global connectivity. In *27th ACIS International Summer Conference on Software Engineering, Artificial Intelligence, Networking and Parallel/Distributed Computing (SNPD 2024)*, pages 157–161. IEEE, 2024.
- [23] Mu Li, XiaoFei Liu, Yong Meng, and QiDi You. A 5g ntn-ran implementation architecture with security. In *2022 4th International Conference on Communications, Information System and Computer Engineering (CISCE)*, pages 42–45. IEEE, 2022.